NEUTRON STAR ATMOSPHERES

G. G. PAVLOV*
Pennsylvania State University, 525 Davey Lab, Universty Park, PA 16802, USA

YU. A. SHIBANOV
Ioffe Physico-Technical Institute, St. Petersburg, 194021, Russia

V. E. ZAVLIN
St. Petersburg Technical University, 195251, Russia

and

R. D. MEYER†
Pennsylvania State University, 525 Davey Lab, University Park, PA 16802, USA

Abstract. We report recent results on the modeling of the atmospheres of cooling neutron stars. The results demonstrate that strong magnetic fields in the atmospheres substantially affect the spectra, angular distribution and polarization of the thermal-like radiation of the neutron stars. In particular, the spectra deviate substantially from both the blackbody spectrum and spectra emitted from nonmagnetic atmospheres. We discuss the application of the results to the interpretation of recently observed soft X-ray spectra of pulsars. Fitting the observed spectra with hydrogen atmosphere models yields neutron star surface temperatures considerably lower than those obtained from the blackbody fits.

Key words: cooling neutron stars, pulsars, stellar atmospheres, X-ray astronomy, ROSAT

1. Introduction

Properties of the thermal-like radiation which stars emit are determined by relatively thin, thermalized plasma layers at the stellar surfaces. These layers are called stellar atmospheres. The atmospheres of "usual" stars have been studied extensively during the last century by both observers and theoreticians. On the contrary, the investigation of the atmospheres of neutron stars has been started only recently, and many unsolved problems still exist in this field. We shall discuss here the modern status of the theory of neutron star atmospheres and the application of the theory to the analysis of observations of thermal-like radiation from pulsars. We will primarily consider the atmospheres of cooling neutron stars since these are the most important for understanding fundamental properties of the superdense matter in neutron star interiors.

There are essentially two factors which make neutron star (NS) atmospheres different from those of usual stars. First is *the immense gravity* at the NS surface. The gravitational acceleration, $g \sim 10^{14} - 10^{15}$ cm s^{-2}, exceeds that for a typical main sequence star by ten orders of magnitude. This means that the NS atmospheres are extremely compressed. The scale height, $\sim kT/m_p g$, typically lies in the range

* On leave from the Ioffe Physico-Technical Institute, St. Petersburg, Russia
† Present address: Yale University, P.O. Box 208101, New Haven, CT 06520, USA

$0.1-100$ cm, *vs.* $\sim 10^8$ cm for a usual star. Typical densities in the NS atmospheres, as we shall see, are $\sim 0.1 - 100$ g cm^{-3}, *vs.* $\sim 10^{-7}$ g cm^{-3}. Due to these high densities, the matter in the NS atmosphere is strongly nonideal. In particular, the nonideality leads to pressure ionization of the matter and to smoothing spectral lines and photoionization edges in the opacities and spectra of the NS radiation. Another important consequence of the high gravity is the stratification of different chemical species in the atmosphere: the upper atmospheric layers should consist of the light elements, e.g. hydrogen and helium, whereas heavier elements should sink down to deeper layers (Alcock and Illarionov, 1980).

Huge magnetic fields, which reach magnitudes up to $10^{11}-10^{13}$ G in the majority of NSs, cause the NS atmospheres to have even more unusual properties. Due to these fields, the NS atmosphere is essentially anisotropic. This means, in particular, that the opacities of the atmospheric matter are quite different from those in usual stars, being strongly dependent on the direction and polarization of radiation. Also, nonuniformity of the magnetic field leads to nonuniform conditions (*e.g.*, nonuniform temperature) along the stellar surface.

Conditions in the NS atmospheres and radiative processes responsible for properties of radiation emitted by NSs in different astrophysical objects depend strongly not only on the magnetic field, but also on the typical temperature of the atmosphere. The temperature, in turn, depends on the history of the object and on the NS environment. Accreting NSs in binaries have rather hot radiating regions, with typical temperatures $\sim 10^8$ K in the *X-ray pulsars*, where accretion is canalized by the very strong magnetic field, and $\sim 10^7$ K in the weakly magnetized *X-ray bursters*. The thermal-like X-ray radiation from the accreting NSs has been widely discussed in recent literature (see Mészáros 1992 and Lewin *et al.* 1993 for a review and references). Here we concentrate on the less-investigated case of *isolated cooling neutron stars*, including *radio pulsars*, whose atmosphere temperatures are substantially lower than those in the accreting NSs, and which emit primarily in the soft X-ray and EUV ranges.

Although the NS atmosphere comprises a negligible part of the NS mass and volume ($\sim 10^{-21}$ and $\sim 10^{-6}$, respectively), it nevertheless determines the properties of the thermal-like radiation. Analysis of the radiation from NSs of different ages allows one to study the thermal evolution of NSs, which is very important for studying still poorly-known fundamental properties of superdense matter in NS interiors. In particular, the cooling rate of NSs essentially depends on the equation of state of nuclear matter, and on the NS mass, radius, magnetic field, and internal composition (Pethick 1992). For instance, for a NS of the age 3×10^5 years, different models predict different surface temperatures in the range $(1-10) \times 10^5$ K (Nomoto and Tsuruta 1987, Shibazaki and Lamb 1989, Page and Applegate 1992, Van Riper and Lattimer 1993, Gnedin and Yakovlev 1993, Umeda *et al.* 1993; and references therein). Lower temperatures are associated with cores of exotic matter, such as pion and kaon condensates or free quarks. In sufficiently massive stars, fast cooling can also be caused by the direct Urca processes involving nucleons. On the other hand, the surface temperature may be increased by the dissipation of the rotational or magnetic energy. Additional reheating may result from the accretion onto the NS surface of particles created in the acceleration gaps of the radio pulsar.

The NS thermal evolution depends crucially on whether nucleon superfluidity occurs (e.g., Page 1993, Levenfish and Yakovlev 1994), which would slow down the direct Urca cooling but would speed up the cooling in the "standard" cooling scenario. The effect of the superfluidity on the NS cooling is determined by the superfluidity transition temperature T_c, below which the nucleons are paired. Different theoretical models give quite different values of T_c, so it would be very important to determine the transition temperature from NS observations.

A number of positive detections of the thermal-like radiation from NSs have been made recently in the soft X-ray range with the EINSTEIN and EXOSAT satellites (Ögelman 1991, and references therein). The most convincing results have been obtained with the ROSAT PSPC for the radio pulsars PSR 0656+14 (Finley *et al.* 1992), PSR 0833-45 (Ögelman *et al.* 1993), PSR 1055-52 (Ögelman and Finley 1993), PSR 1929+10 (Yancopoulos *et al.* 1993), and PSR J0437-4715 (Becker and Trümper 1993), and for the γ-ray pulsar Geminga (Halpern and Ruderman 1993). A detailed review of these observations is given by Ögelman (1994). Here we only mention that almost all of the above objects show two-component spectra. The soft component probably originates from the whole NS surface. Fitting this with the *blackbody* spectrum gives a (blackbody) temperature in the range $2 \times 10^5 - 2 \times 10^6$ K for different objects, and generally, older pulsars have lower temperatures, as expected. The origin of the hard component remains questionable. It may be generated either in the pulsar polar caps which are heated by the accretion of relativistic particles created in the pulsar acceleration gaps, or by nonthermal particles in pulsar magnetospheres or surrounding nebulae. Blackbody fits of the hard components give temperatures $\sim (2-4) \times\ 10^6$ K, approximately the same for all the objects for which the hard components were observed. Radiation in both the soft and hard components show pulsations, with the energy-dependent pulsed fraction $\lesssim 10-30\%$. The pulse phases also seem to depend on the photon energy, since the pulsations in the soft and hard components are always substantially phase-shifted.

To interprete these and future observations in terms of the surface temperature, it is necessary to take into account that the spectrum emitted by the NS surface may deviate substantially from the blackbody spectrum due to the presence of a plasma atmosphere. In other words, *thermal-like radiation is not blackbody radiation*; *neutron stars are not perfect blackbody emitters.* Since the temperature in the atmosphere varies with depth, and the photon mean free path depends upon the photon energy, the emitted spectra do not correspond to any definite temperature. If the atmosphere consists mainly of light elements, high-frequency radiation escapes from deeper and hotter layers, giving rise to a hard spectral tail in excess of the Wien dependence for the same effective temperature $T_{\rm eff}$ (see, e.g., Mihalas 1978). This obviously may lead to a substantial overestimation of the effective surface temperature when interpreting the X-ray spectra in terms of blackbody radiation (Romani 1987). A bright example has been presented by Finley *et al.* (1992). They demonstrated that the blackbody fit of the ROSAT spectrum of PSR 0656+14 yields $T_{\rm eff} \sim\ 9 \times\ 10^5$ K whereas fitting with Romani's model spectrum of the *non-magnetic* helium atmosphere results in $T_{\rm eff} \sim 3 \times 10^5$ K; this factor of 3 difference leads to quite different conclusions concerning the NS cooling models.

In the case of atmospheres with strong magnetic fields the picture looks more complicated. Due to the anisotropy of the magnetized atmosphere, radiation there propagates as two so-called *normal modes* with different (almost orthogonal) polarizations and opacities (see, *e.g.*, Gnedin and Pavlov 1974). Moreover, properties of the outgoing radiation are mainly determined (Pavlov and Shibanov 1978) by the "extraordinary" mode; its opacity is much lower (*i.e.*, photon mean free path much longer) than the "ordinary" mode opacity if the photon and thermal energies, $\hbar\omega$ and kT, are much lower than the electron cyclotron energy $\hbar\omega_B = \hbar eB/m_ec = 11.6(B/10^{12}\mathrm{G})$ keV. Generally, the extraordinary mode opacity decreases with ω slower than the opacity for no magnetic field. This means that the emitted spectrum for a strong magnetic field should be closer to the blackbody spectrum than in the field-free case. This fact was recognized by Shibanov *et al.* (1992) who considered model NS atmospheres assuming that they are fully ionized, so that the opacities are only due to free-free transitions and Thomson scattering, which can be justified for sufficiently high effective temperatures, $T_{\mathrm{eff}} \gtrsim 10^6$ K. The same conclusion was drawn by Miller (1992) who used polarization-averaged bound-free opacities assuming other sources of the opacity to be unimportant.

Shibanov *et al.* (1993a) presented preliminary results of modeling magnetic, partially ionized atmospheres with proper allowance for the anisotropic photon diffusion in two polarization modes. We describe in more detail the physical processes in the NS atmospheres in Section 2, and present recent results of the modeling in Section 3. Applications to the interpretation of soft X-ray observations of NSs, and some problems to be solved for a better understanding of the NS atmospheres, are discussed in Section 4.

2. Basic Equations and Physical Input

2.1. Radiative transfer

The transfer of polarized radiation in a strongly magnetized plasma can be described (Gnedin and Pavlov 1974) in terms of two coupled equations for the specific spectral intensities I_j of two normal (polarization) modes:

$$\mu\frac{dI_j(\mathbf{n})}{dy} = K_j(\mathbf{n})I_j(\mathbf{n}) - \sum_{i=1}^{2}\int d\mathbf{n}' I_i(\mathbf{n}')K^s_{ij}(\mathbf{n}',\mathbf{n}) - K^a_j(\mathbf{n})\frac{B_\omega(T)}{2}\,, \qquad (1)$$

where $\mu = \cos\Theta$ is the cosine of the angle between the wave vector direction $\mathbf{n}$ and the normal $\mathbf{N}$ to the surface of the atmosphere, y is the depth in the atmosphere (in g cm^{-2}), $B_\omega(T)$ is the Planck function, and $j = 1$ and 2 are the indices of the extraordinary and ordinary modes, respectively. The total opacity K_j is the sum of the absorption and scattering opacities,

$$K_j(\mathbf{n}) = K^a_j(\mathbf{n}) + K^s_j(\mathbf{n})\,, \qquad (2)$$

and the scattering opacity is

$$K^s_j(\mathbf{n}) = \sum_{i=1}^{2}\int d\mathbf{n}' K^s_{ij}(\mathbf{n}',\mathbf{n})\,, \qquad (3)$$

where $K^s_{ij}(\mathbf{n}', \mathbf{n})$ describes scattering from the ith mode to the jth mode; these modes propagate in the directions $\mathbf{n}'$ and $\mathbf{n}$, respectively.

Because of the sharp angular dependence of the opacities, the numerical solution of Equation (1) is rather complicated. For the radiative energy spectral densities $(4\pi/c)J_j$, much simpler diffusion-type equations can be obtained (Kaminker *et al.* 1982a):

$$\frac{d}{dy} D_j \frac{dJ_j}{dy} - S(J_j - J_{3-j}) = \kappa_j \left(J_j - \frac{B_\omega(T)}{2} \right) , \tag{4}$$

where the frequency-dependent coefficients κ_j and S are, respectively, the angle-averaged absorption opacity of the mode j and the mode conversion coefficient;

$$\kappa_j = \frac{1}{4\pi} \int d\mathbf{n}\, K^a_j(\mathbf{n}), \qquad S = \frac{1}{4\pi} \int d\mathbf{n}\, d\mathbf{n}'\, K^s_{12}(\mathbf{n}, \mathbf{n}'). \tag{5}$$

Due to the anisotropy of the medium, the photon mean free path (diffusion coefficient) D_j is a function of the angle Θ_B between the magnetic field $\mathbf{B}$ and the normal $\mathbf{N}$:

$$D_j = D^{\|}_j \cos^2 \Theta_B + D^{\perp}_j \sin^2 \Theta_B \, , \tag{6}$$

$$D^{\|}_j = \int_0^1 \frac{\mu^2 d\mu}{K_j(\mu)} , \quad D^{\perp}_j = \frac{1}{2} \int_0^1 \frac{(1-\mu^2) d\mu}{K_j(\mu)} \, . \tag{7}$$

To ensure the continuity of the normal flux component,

$$F_j = \int d\mathbf{n}\, \mu I_j(\mathbf{n}) \simeq 4\pi D_j \frac{dJ_j}{dy} \, , \tag{8}$$

and the absence of externally incident radiation, the radiation field must satisfy the following boundary conditions:

$$2D_j \frac{dJ_j}{dy} = J_j \quad \text{for } y = 0; \qquad\qquad J_j \to \frac{1}{2} B_\omega(T) \quad \text{for } y \to \infty. \tag{9}$$

Once Equation (4) is solved, one can find the spectral flux from Equation (8) and the specific intensity from the equation

$$I_j(\mathbf{n}) = \int_0^\infty \frac{dy}{\mu} \left[\frac{B_\omega(T)}{2} K^a_j + \sum_{j=1}^{2} K^s_{ji} J_j \right] \exp \left(- \int_0^y K_j \frac{dy}{\mu} \right) , \tag{10}$$

where $K^s_{ji} = \int d\mathbf{n}'\, K^s_{ji}(\mathbf{n}, \mathbf{n}')$. It should be stressed that even if we were not interested in the polarization of the emitted radiation, the total (polarization-summed) flux and intensity ($F = F_1 + F_2$ and $I = I_1 + I_2$) cannot be found without solving the transfer equations for *polarized* radiation.

Results obtained with the diffusion approach presented above can be used as a first approximation for a subsequent iterational procedure which would converge to a solution having a more accurate spectrum and angular dependence for the outgoing radiation. Shibanov *et al.* (1994) show that, for conditions of interest, the "exact" total flux and intensity are very close to those obtained with the above diffusion approximation. Significant differences between the diffusion approximation and exact results are seen only in the ordinary mode, which gives only a minor contribution to the total flux at the frequencies of interest.

2.2. Opacities

The transfer coefficients are generally determined by free-free, bound-free and bound-bound transitions, and by Thomson scattering (Comptonization effects can be neglected at $T \lesssim 10^7$ K). In particular, the general structure of the opacity caused by any of these processes appears in the dipole approximation as

$$K_j^{(x)}(\omega, \vartheta) = \sum_{\alpha=-1}^{1} k_\alpha^{(x)}(\omega) a_\alpha^j(\omega, \vartheta)\,, \tag{11}$$

where ω is the photon frequency, ϑ is the angle between the wave vector and the magnetic field, the superscript x denotes the radiative process, and $a_\alpha^j(\omega, \vartheta)$ is the squared modulus of the cyclic projection of the normal mode polarization unit vector into the coordinate system with the z-axis along $\mathbf{B}$:

$$a_0^j = \frac{\sin^2\vartheta}{2}(1 + p_Q^j), \qquad a_{\pm 1}^j = \frac{1}{4}(1 + \cos^2\vartheta \pm 2p_V^j \cos\vartheta - p_Q^j \sin^2\vartheta)\,, \tag{12}$$

where p_V^j and p_Q^j are the degrees of the circular and linear normal mode polarizations, respectively. The coefficients $k_\alpha^{(x)}$ in Equation (11) do not depend on ϑ and are determined by the specific process; $k_0^{(x)}$ is the opacity for radiation propagating perpendicular to the magnetic field and linearly polarized along the field, and $k_\pm^{(x)}$ are the opacities for circularly polarized radiation propagating along the field.

The *free-free transitions of electrons* and *Thomson scattering on electrons* in a magnetized plasma have been investigated in detail by Kaminker *et al.* (1982b, 1983). For these processes

$$k_\alpha^{(s,e)} = \frac{N_e \sigma_T}{\rho} \frac{\omega^2}{(\omega + \alpha\omega_B)^2 + (\gamma_r + \gamma_\alpha)^2} \quad \text{and} \quad k_\alpha^{(ff,e)} = k_\alpha^{(s,e)} \frac{\gamma_\alpha}{\gamma_r}\,, \tag{13}$$

where N_e is the electron number density, σ_T is the Thomson cross section, $\gamma_r = (2/3)\omega^2(e^2/m_e c^3)$ is the radiative (natural) width, and $\gamma_0 = \gamma_\|$ and $\gamma_{+1} = \gamma_{-1} = \gamma_\perp$ are the longitudinal and transverse effective frequencies of electron-ion collisions in a strong magnetic field as investigated by Pavlov and Panov (1976). If the Doppler width of the cyclotron resonance, $\gamma_D = \omega_B(kT/m_e c^2)^{1/2}|\cos\vartheta|$, exceeds $\gamma_\alpha + \gamma_r$, equations (13) are valid for frequencies not too close to the resonance, $|\omega - \omega_B| \gg \gamma_D$ (the cold plasma approximation). Notice that in the most interesting frequency range $\omega \ll \omega_B$ the opacities for the transverse polarizations are much less than those for the longitudinal polarization, i.e., $k_{\pm 1} \ll k_0$.

For photon energies below or around the ion cyclotron energy, $\hbar\omega \lesssim \hbar\omega_{Bi} = (Zm_e/Am_p)\hbar\omega_B = (Z/A)\hbar\omega_{Bp} = 6.3(Z/A)B_{12}$ eV, where Ze and $Am_p = m_i$ are respectively the charge and mass of the ion, *Thomson scattering on ions* and the *free-free transitions of ions* may also be important. In a relaxation-time approximation, the opacities read

$$k_\alpha^{(s,i)} = \frac{N_i \sigma_T}{\rho}(Z^2\mu)^2 \frac{\omega^2}{(\omega - \alpha\omega_{Bi})^2 + \mu^2(Z^2\gamma_r + \gamma_\alpha)^2} \quad \text{and} \quad k_\alpha^{(ff,i)} = k_\alpha^{(s,i)} \frac{\gamma_\alpha}{Z^2\gamma_r}\,, \tag{14}$$

where N_i is the ion number density and $\mu = m_e/m_i$.

For the *bound-free transitions* (photoionization) we have

$$k_\alpha^{(bf)} = \frac{N_a}{\rho} \sum_{s,n} p_{sn} \sigma_{sn}^\alpha \,, \tag{15}$$

where N_a is the number density of atoms; $s = 0, 1, 2, \ldots$ is the negative of the projection of the angular momentum of the atom onto $\mathbf{B}$; $n = 0, 1, 2, \ldots$ is the longitudinal quantum number of the atom in a strong magnetic field (see, e.g., Canuto and Ventura 1977); p_{sn} is the population of the state $\{s, n\}$; and σ_{sn}^α is the photoionization cross section for the corresponding polarization. The cross sections of the *isolated hydrogen atom* for $\alpha = 0, \pm 1$ have been found by Potekhin and Pavlov (1993). Since the binding energies of the magnetized atom are much larger than in the field-free case (e.g., ionization potentials for the hydrogen ground state are $\sim 100 - 300$ eV in typical magnetic fields of NSs), the photoionization thresholds move into the soft X-ray range. For the longitudinal polarization ($\alpha = 0$), the threshold value of the cross section and the cross section's dependence on the frequency above the threshold are close to those for no magnetic field. For the transverse polarizations ($\alpha = \pm 1$), the threshold values are lower by 3 – 4 orders of magnitude, and the cross sections have a slower decrease with increasing frequency.

Polarization-averaged photoionization cross sections of heavier atoms were calculated by Miller and Neuhauser (1991). To our best knowledge, nobody has investigated the photoionization of the heavy atoms in strong magnetic fields by polarized radiation. Moreover, it seems that the structure of magnetized atoms more complex than hydrogen-like ions is still not sufficiently understood, so that it is, perhaps, premature to include these in the magnetic atmosphere models. Thus, only *hydrogen atmospheres* are discussed below.

In a dense NS atmosphere each atom is strongly influenced by surrounding particles which may distort the levels of the atom and dissolve them into the continuum. To take into account these *nonideality* (or pressure) effects, one can generalize an approach which had been developed by Däppen *et al.* (1987) and Hummer and Mihalas (1988) for a nonmagnetized plasma. This approach is based on the so-called *occupation probability formalism*, in which the population of each level is multiplied by a density-dependent occupation probability w_{sn}:

$$p_{sn} = \frac{1}{U} w_{sn} \exp\left(\frac{\chi_{sn} - s\hbar\omega_{Bp}}{kT}\right) \,, \tag{16}$$

where $-\chi_{sn}$ is the (negative) eigenvalue of the one-dimensional (longitudinal) Schrödinger equation, the term $\hbar\omega_{Bp}$ takes into account the effect of the finite mass of the proton on the energies of the atomic states (Herold *et al.* 1981), and

$$U = \sum_{s,n=0}^{\infty} w_{sn} \exp\left(\frac{\chi_{sn} - s\hbar\omega_{Bp}}{kT}\right) \tag{17}$$

is the internal partition function. For the temperatures of interest, the levels are mainly affected by electric microfields of surrounding ions. The occupation probabilities are determined by the distribution function of the electric microfields $W(\beta)$,

$$w_{sn} = \int_0^{\beta_{sn}^{\rm cr}} {\rm d}\beta\, W(\beta)\ , \qquad \beta_{sn}^{\rm cr} = 0.042 \left(\frac{\chi_{sn}}{\rm Ry}\right)^2 (N_i a_B^3)^{-2/3}\ , \tag{18}$$

where β is the electric microfield in units of the Holtsmark field, $\beta_{sn}^{\rm cr}$ is the critical value of the electric field which destroys the atom, Ry = 13.6 eV is the Rydberg energy, and a_B is the Bohr radius. The numerical coefficient in the equation for $\beta_{sn}^{\rm cr}$ is a factor of $\sqrt{3}$ larger than in the corresponding equation for the field-free case; this approximately accounts for the fact that only the longitudinal (with respect to the magnetic field) component of the electric field is able to ionize the strongly magnetized atom.

Besides reducing the population of the atomic levels, the electric fields of surrounding ions can lower the photoionization thresholds, leading to the smoothing of photoionization edges in the opacity spectra. Following Däppen *et al.* (1987), we included this effect, using

$$\sigma_{sn}^{\alpha} = \sigma_{sn}^{\alpha,{\rm iso}} \left(1 - \frac{w_{sn}^{\alpha}}{w_{sn}}\right) \tag{19}$$

instead of the cross section $\sigma_{sn}^{\alpha,{\rm iso}}$ for the isolated atom. In Equation (19) $w_{sn}^{\alpha} = 0$ for $\hbar\omega > \chi_{sn} + \alpha\omega_{Bp}$, i.e., the cross section is not changed above the unperturbed threshold, and

$$w_{sn}^{\alpha} = \int_0^{\beta_{sn}^{\alpha}} d\beta\, W(\beta)\,, \qquad \beta_{sn}^{\alpha} = \beta_{sn}^{\rm cr}\left(1 - \frac{\hbar\omega}{\chi_{sn} + \alpha\omega_{Bp}}\right) \tag{20}$$

for $\hbar\omega < \chi_{sn} + \alpha\omega_{Bp}$. Equations (19) and (20) imply that the cross section below the unperturbed threshold remains finite, varying smoothly with frequency. The values of $\sigma_{sn}^{\alpha,{\rm iso}}$ below the threshold are obtained by a smooth extrapolation of the above-threshold frequency dependence.

The *bound-bound transitions* of the strongly magnetized atoms can also make a significant contribution to the opacity. However, only the oscillator strengths of the transitions in atoms at rest have been investigated in detail (Forster *et al.* 1984). The coupling of the center-of-mass motion of the atom to its internal structure, not considered by Forster *et al.*, affects substantially the oscillator strengths (Potekhin 1993) and leads to very strong spectral line broadening (Pavlov and Mészáros 1993). Investigation of the coupling effect on the bound-bound transitions is in progress now (Potekhin and Pavlov 1994), but the results have not yet been included in the atmosphere models.

To obtain the opacity with allowance for many processes, one can merely add the coefficients $k_{\alpha}^{(x)}$ for these processes and substitute the sum into Equation (11). A more complicated situation is with the polarization coefficients a_{α}^{j} (or p_V^j and p_Q^j) which depend nonlinearly on the contributing processes. To compute these, one should know the medium polarizability tensor (Pavlov *et al.* 1980). The tensor is well known for the fully ionized plasma, and the normal mode polarizations have been thoroughly investigated for the case when only the free-free transitions and Thomson scattering are important (Kaminker *et al.* 1982b, 1983). These polarizations were used for modeling fully ionized atmospheres (Shibanov *et al.* 1992). However, neither polarizability nor normal mode polarization have been investigated for the case when nonionized, strongly magnetized atoms make a substantial contribution to opacity. Based on general considerations, one can only argue that the normal mode polarizations should be almost linear at $\omega \ll \omega_B$, one being perpendicular to the magnetic field and the other lying in the "wave vector - magnetic field" plane, unless the angle ϑ is very close to zero or π. So, at the present moment, one can either assume that the polarizations are *exactly linear* or use the polarizations derived for the fully ionized plasma. An analysis shows (Shibanov *et al.* 1993b) that these two assumptions may lead to a noticeably different angular dependence of the specific intensity, especially at small ϑ where admixture of the circular polarization is important, but they result in almost the same emitted spectrum. The assumption that the normal mode polarizations are exactly linear strongly simplifies the equations for the transfer coefficients. For instance, the normal mode opacities are then expressed in terms of k_α as

$$K_1 = \frac{1}{2}(k_{+1} + k_{-1}), \qquad K_2 = k_0 \sin^2\vartheta + \frac{\cos^2\vartheta}{2}(k_{+1} + k_{-1})\,. \tag{21}$$

Notice that the opacity K_1 of the extraordinary mode is isotropic and contains only transverse opacities $k_{\pm 1}$ which are much smaller than k_0. This means that $K_1 \ll K_2$ for a wide range of ϑ. An example of the spectral dependence of the photon mean free paths D_1 and D_2 for $B = 2.35 \times 10^{12}$ G is shown in the left panel of Figure 1. We see that $D_1 \gg D_2$. The extraordinary photons are strongly absorbed around the ion cyclotron energy, $\hbar\omega_{Bp} \simeq 15$ eV. Broad absorption features at $\hbar\omega_B \sim 0.1 - 0.2$ keV are caused by the photoionization of the hydrogen atom, the features being more strongly smoothed by interaction with surrounding ions at higher densities. Both D_1 and D_2 grow monotonously with ω at $\hbar\omega \gtrsim 0.2$ keV.

2.3. Thermal, hydrostatic and ionization equilibrium

To solve the radiative diffusion equations, one must know how the temperature and densities of atoms, ions and electrons depend on the depth. These dependencies can be found from the equations of thermal, hydrostatic and ionization equilibrium supplemented by the equation of state of the atmospheric matter. We consider atmospheres in radiative thermal equilibrium which requires the outward flux to remain constant throughout the atmosphere, *i.e.*,

$$4\pi \int d\omega \left(D_1 \frac{dJ_1}{dy} + D_2 \frac{dJ_2}{dy} \right) = \sigma T_{\rm eff}^4\,, \quad \text{or} \quad \int d\omega \sum_j \kappa_j \left(J_j - \frac{1}{2} B_\omega(T) \right) = 0 \ , \tag{22}$$

where $T_{\rm eff}$ is the effective temperature. These equations imply that other heat transport mechanisms (e.g., electron heat conductivity), as well as additional sources of energy release, are of no importance. Generally, this is the case in the nondegenerate outer layers of non-accreting neutron stars. However, one should bear in mind that the assumption of convective stability as implied here may, in principle, be violated at sufficiently high temperature gradients, and it is to be checked for each calculated model.

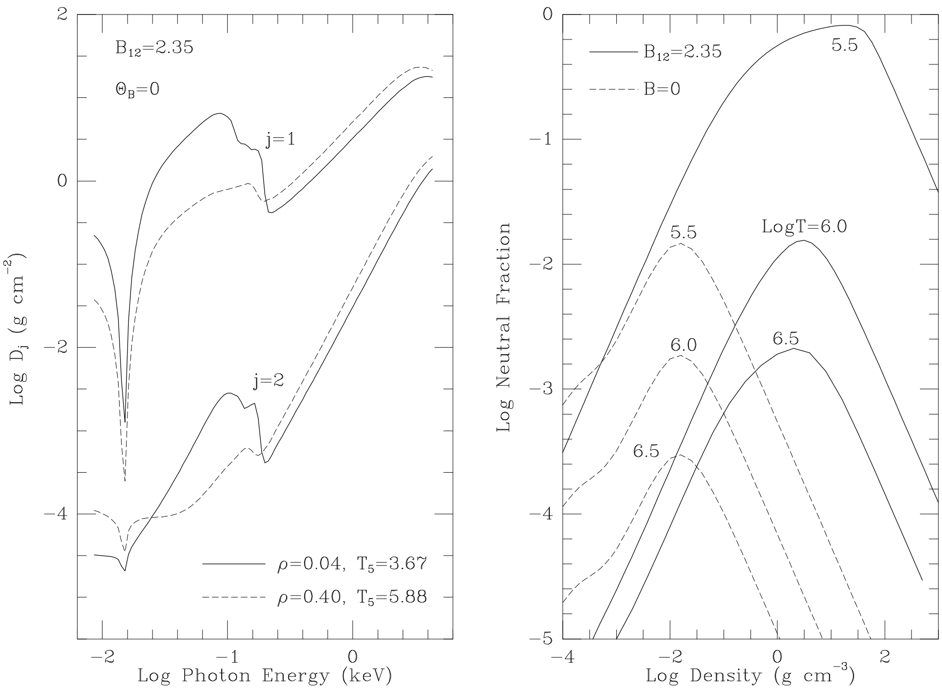

Fig. 1. **Left**: Photon mean free paths of the extraordinary (j=1) and ordinary (j=2) modes in a magnetized hydrogen plasma for two combinations of the density ρ (in g cm^{-3}) and temperature T (in K). **Right**: Fraction of neutral hydrogen atoms *vs.* density for different temperatures.

Hydrostatic equilibrium further requires that $\mathrm{d}P/\mathrm{d}y = g$, where g is the gravitational acceleration which can be considered to be constant throughout the atmosphere (its typical values are $\sim (0.5-5)\times 10^{14}$ cm s^{-2}). The pressure P generally consists of the gas, radiation and magnetic components. The radiation pressure can be neglected if the luminosity is much lower than the Eddington luminosity, which is true for $T_{\rm eff} \ll 10^7$ K. The magnetic pressure equals zero in force-free magnetic fields, *e.g.*, in the uniform or dipole fields. The NS atmosphere is very thin, so the magnetic field should be almost uniform there. On the other hand, even a small nonuniformity in the field may significantly affect the hydrostatic equilibrium. Since we do not know the real geometry of the magnetic field in the atmosphere, we assume that it is locally uniform so that only the gas pressure becomes important. For the gas pressure we adopt the equation of state for an ideal nondegenerate gas, $P = (N_a + N_e + N_p)kT$. Although the nonideality of the partially ionized plasma changes the equation of state in dense NS atmospheres, the corrections are small, and nonideality effects are less important than for ionization equilibrium and for opacity spectra. At low effective temperatures the electron gas may be partially degenerate in deep atmospheric layers; however, the degeneracy is mostly suppressed by the strong magnetic field so that we neglect this also.

To close the system of atmosphere modeling equations, one must add an equation for the ionization equilibrium. It was shown by Gnedin *et al.* (1974) that a strong magnetic field substantially affects the degree of ionization. First, it increases the ionization potentials for $\hbar\omega_B \gg \mathrm{Ry}$ ($B \gg 10^9$ G) and thereby reduces the degree of ionization at a given T and ρ. Second, it increases the volume of the phase space occupied by electrons at $\hbar\omega_B \gtrsim kT$ (quantization of the transverse electron motion), which enhances ionization. At very high magnetic fields, $\hbar\omega_{Bp} \gtrsim kT$, quantization of the proton motion is also important (Khersonskii 1987). To calculate the ionization equilibrium, one can include the nonideality (pressure) effects into the atomic partition function U (see Eq. [17]), and use the modified Saha equation

$$N_a = N_e\, N_p\, \frac{1}{2} \left(\frac{2\pi\hbar^2}{m_e kT}\right)^{3/2} \frac{\tanh\eta_e}{\eta_e}\, \frac{\sinh\eta_p}{\eta_p}\; U\,, \tag{23}$$

where $\eta_e = \hbar\omega_B/kT$, $\eta_p = \hbar\omega_{Bp}/kT$. An example of ionization equilibrium in the magnetized and field-free plasmas is shown in Figure 1. The occupation probabilities here were calculated for the Holtsmark distribution of the electric microfields. We see that a strong magnetic field substantially increases the nonionized fraction at densities and temperatures typical for the NS atmospheres. Since magnetized atoms have much higher binding energies, the pressure ionization occurs at higher densities ($\rho \gtrsim 3-30$ g cm^{-3} *vs.* $0.01-0.03$ g cm^{-3} in the field-free case).

The above system of equations can be solved numerically by obviously generalizing to the case of two polarization modes the well-known methods for modeling stellar atmospheres (Mihalas 1978). Some details can be found in the papers by Zavlin and Shibanov (1991), Shibanov *et al.* (1992), and Shibanov *et al.* (1994). Quite generally, one should use an iteration procedure which starts with some approximation of the temperature as a function of depth (usually, the Eddington approximation for grey atmospheres). Given the temperature profile, one can compute hydrostatic and ionization equilibria, find opacities, and solve the radiative transfer equations. This solution is applied to find corrections ΔT to the temperature in each atmospheric layer using the radiative equilibrium condition. Then the procedure is repeated until temperature convergence is reached. To compute the models presented below, we typically used a 100×100 grid of logarithmically spaced depths and energies, and iterated until $\Delta T/T \lesssim 1\%$.

3. Results

3.1. Spectra of local fluxes

Figures 2 and 3 show spectra of the polarization-summed local fluxes $F = F_1 + F_2$ at $y = 0$ (see Eq. [8]) emitted by an element at the NS surface for different values of the model parameters $T_{\rm eff}$, B, Θ_B, and g. Figure 2 shows how the spectra depend on the value of the magnetic field for the effective temperatures $T_{\rm eff} = (3.2-15.6)\times 10^5$

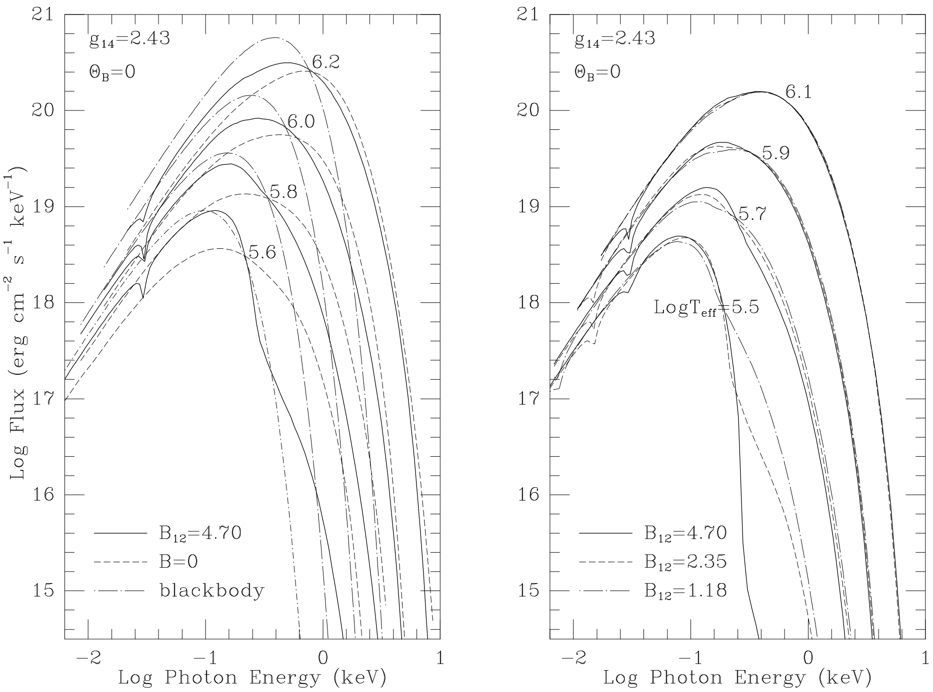

Fig. 2. Spectra of local fluxes emerging from hydrogen atmospheres for different effective temperatures and magnetic fields.

K. The spectra were computed for the gravitational acceleration $g = 2.43 \times 10^{14}$ cm s^{-2}, which corresponds to the "canonical" NS mass and radius, $M = 1.4M_\odot$ and $R = 10$ km, and for the magnetic field oriented along the normal to the NS surface. We see that all of the model spectra are significantly *harder* at high frequencies than the blackbody spectra for the same $T_{\rm eff}$. On the other hand, all of the "magnetic" spectra are somewhat *softer* at high frequencies than the corresponding non-magnetic spectrum (obtained by the same method we have described). This is because, for the magnetic case, the mean free path D_1 of the extraordinary mode (which is responsible for the flux spectrum in a wide range of frequencies) depends on frequency more gradually than that at $B = 0$ (see Fig.1). Since the shape of the outgoing spectrum is determined by the slope of the extraordinary opacity spectrum more than by its absolute value, the spectra for the highest effective temperatures only slightly depend on B. At lower $T_{\rm eff}$, the photoionization becomes important, and the spectra are more field-dependent. In particular, a wide, smooth depression seen at $\hbar\omega \sim 0.1 - 0.3$ keV in the low-temperature spectra is a superposition of

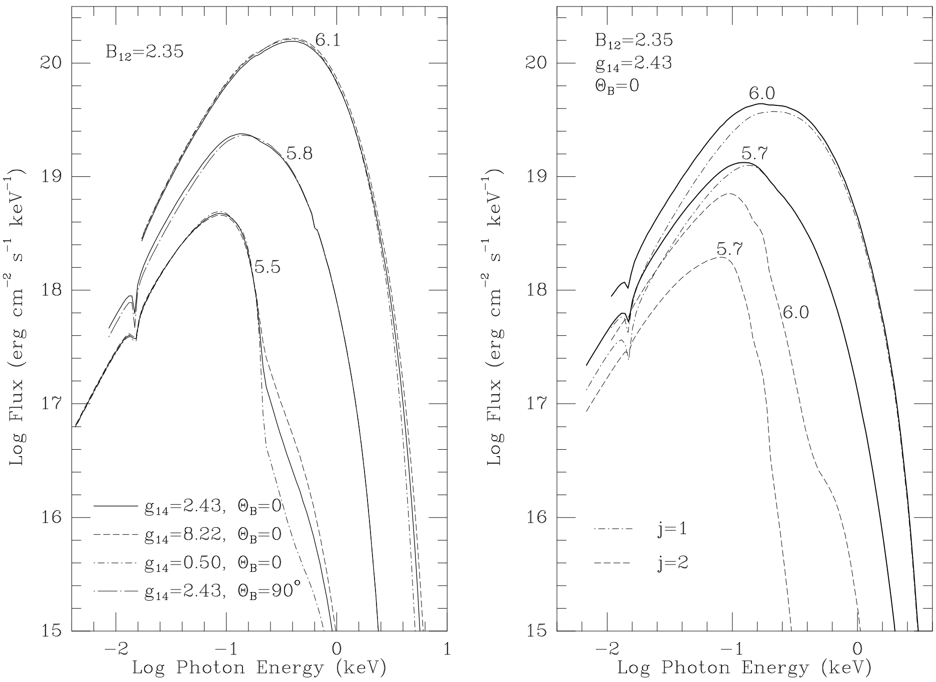

Fig. 3. **Left**: Effect of the gravity and orientation of the magnetic field on the local spectral fluxes. **Right**: Spectral fluxes in two polarization modes.

the *photoionization edges* of the strongly magnetized hydrogen atoms redshifted and smoothed by the pressure effects. The field dependence is most vividly displayed in the *proton cyclotron absorption lines* centered at frequencies ω_{Bp} (the electron cyclotron lines lie far into the Wien tails of the spectra at these temperatures and are not seen in the graphs). At low frequencies, the model spectra approximately follow the Rayleigh-Jeans law corresponding to a characteristic surface temperature falling systematically below the value of $T_{\rm eff}$. The spectral dependence on B means that if a rotating NS exposes surface areas with different magnetic fields, the NS radiation should be modulated with the rotation period, the pulse fraction being dependent on the photon energy. It is interesting that at a given $T_{\rm eff}$ the spectra for different magnetic fields cross each other and the Planck spectrum at approximately the same energy, $\hbar\omega \simeq (5-7)kT_{\rm eff}$. This means that there should exist a *crossover energy* in the phase-dependent spectra such that pulsations above and below this energy are phase-shifted by 180°. Since the photon mean free paths depend on the *orientation of the magnetic field* with respect to the normal to the atmosphere (angle Θ_B), there should also exist a difference in spectra escaping from regions with magnetic fields of the same magnitude but different orientation. In fact, the difference appears to be quite small, which is demonstrated on the left panel of Figure 3 for $\log T_{\rm eff} = 5.8$. This can be explained by the fact that the mean free path of the extraordinary mode is isotropic (see Eq. [21]) in the adopted approximation of linearly polarized normal modes. Using exact (still unknown) normal mode polarizations may lead to flux spectra which are more anisotropic, as demonstrated by Ventura *et al.* (1993) for the case of fully ionized atmospheres.

The left panel of Figure 3 also shows the dependence of the flux spectra on the *gravitational acceleration*. We see that at high $T_{\rm eff}$ the effect of gravity is hardly visible, whereas at low $T_{\rm eff}$ it is much more noticeable. This effect is primarily associated with how the pressure affects the photoionization opacities: the density in the atmosphere is greater, and the smoothing of the photoionization edges is more pronounced, at higher gravities (*cf.* Zavlin *et al.* 1993).

The right panel of Figure 3 demonstrates another major feature of the cooling NS radiation: the high degree of its *polarization*. It arises due to the fact that the extraordinary mode (polarized perpendicular to $\mathbf{B}$) escapes from deeper and hotter layers than the ordinary mode. The degree of polarization is especially high at high frequencies; the intensities of the ordinary and extraordinary modes are similar at low frequencies, although the extraordinary flux exceeds the ordinary one everywhere except in the vicinity of the proton cyclotron feature. As shown by Ventura *et al.* (1993) for the fully ionized atmospheres, the radiation in the ordinary mode is more sensitive to the orientation of the magnetic field since the orientation effect on the temperature profile is more pronounced in outer layers than in deeper ones (see the discussion of Figure 4 below). The spectral features associated with the bound-free transitions are seen more clearly in the ordinary mode since it escapes from less dense layers.

3.2. Structure of the NS atmospheres

For a better understanding of the properties of the emitted radiation it is useful to examine the structure of the NS atmospheres. For the escaping radiation, the most important feature is the *temperature profile* in the atmosphere. The left panel of Figure 4 shows the profiles for two values of $T_{\rm eff}$ and different values of the magnetic field, including $B = 0$. In very deep layers, where T significantly exceeds $T_{\rm eff}$, all the profiles follow the Eddington law, $T = 0.93 T_{\rm eff} \tau_R^{1/4}$, where τ_R is the Rosseland optical depth. The curves for $B = 0$ lie above the "magnetic" curves because the same layers correspond to a lower Rosseland depth in the magnetic field than in the field-free case. The magnetic temperature profiles show a local *flattening* at depths where $T \simeq T_{\rm eff}$, which lie at $\tau_R \lesssim 1$. Above these layers the atmosphere is transparent for the extraordinary mode at energies $\hbar\omega \gtrsim (3-5)kT$ which correspond to the maxima of the spectral fluxes (see Figs. 2 and 3). However, the atmosphere remains opaque for the ordinary mode which determines the temperature profile in outer layers. So, the curves continue to decrease with decreasing y after the local flattening until the temperature reaches its "surface" value T_s. The *surface temperature* decreases slightly with increasing B, remaining comparable with that for $B = 0$. Notice that typical values of $T_s \simeq (0.3-0.5) T_{\rm eff}$ are noticeably lower than

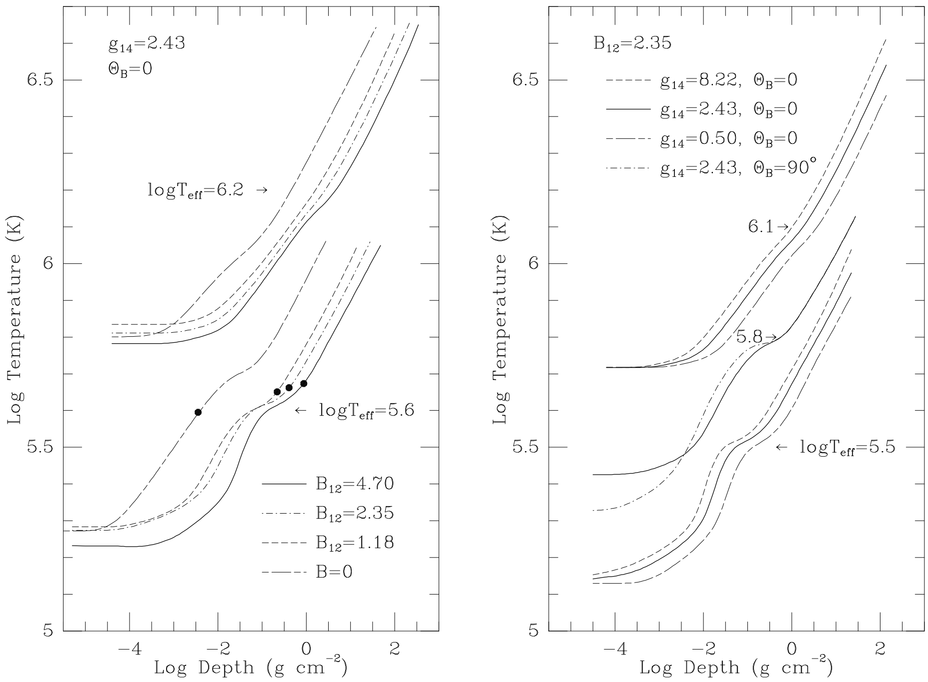

Fig. 4. Temperature profiles in hydrogen atmospheres for different model parameters. The filled circles on the curves show the temperatures at $\tau_R = 1$ for $\log T_{\rm eff} = 5.6$.

$T_s = 0.84 T_{\rm eff}$ for the grey atmosphere. The right panel of Figure 4 demonstrates the dependence of the temperature profiles on g and Θ_B. The effect of gravity is comparable in scale to that of the magnetic field, although T_s is almost independent of g. On the contrary, T_s decreases by 20–30% when Θ_B increases from 0 to 90°. This means, in particular, that *the NS surface is cooler on the magnetic equator than on the poles* (at the same $T_{\rm eff}$), which should lead to pulsed low-frequency (UV and optical) NS radiation.

Figure 5 shows the density profiles and the degree of ionization profiles in the NS atmospheres. As expected, the density grows monotonously with the depth. The density at a given depth grows with increasing B and g, and decreases with increasing $T_{\rm eff}$. The value of ρ at $\tau_R = 1$ increases with B ($\sim 0.1 - 10$ g cm^{-3} for $B \sim 10^{12} - 10^{13}$ G vs. $0.003 - 0.3$ g cm^{-3} for $B = 0$), *i.e., magnetic atmospheres are denser than nonmagnetic ones.* The right panel of Figure 5 demonstrates that strong magnetic fields considerably reduce the ionization in the layers responsible for the emission of soft X-ray radiation. This means, in particular, that the pho-

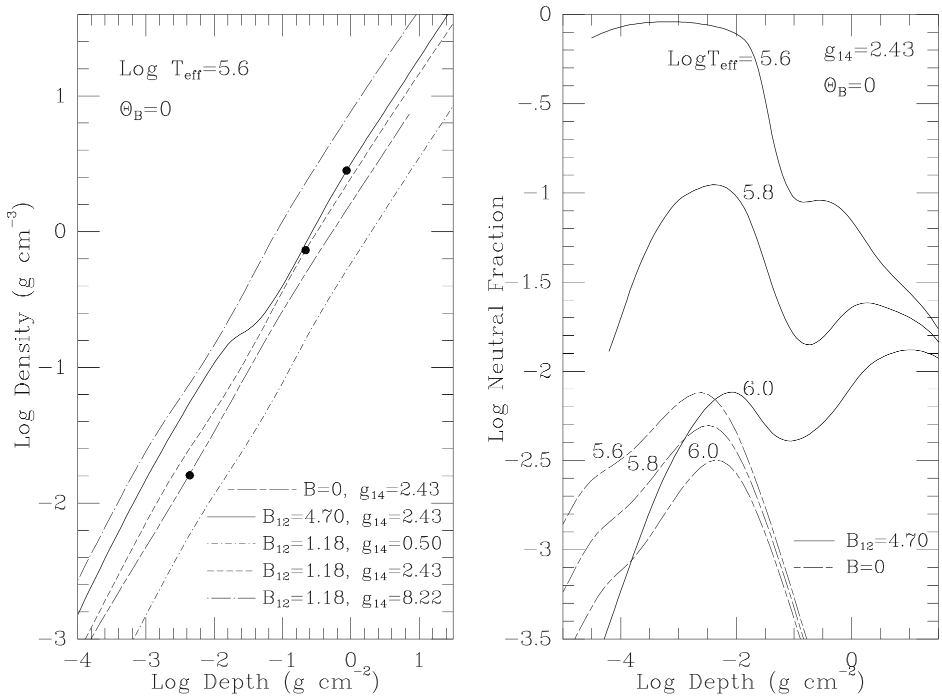

Fig. 5. Dependence of the density and hydrogen neutral fraction on the depth. The filled circles show the densities at $\tau_R = 1$ for $g = 2.43 \times 10^{14}$ cm s^{-2}.

toionization of magnetized hydrogen atoms is the main contributor to opacity above the photoionization thresholds, even at comparatively high temperatures.

3.3. Radiation integrated over the visible NS surface

The radiation from a NS surface element in a given direction is described by the outgoing specific flux $I \cos\Theta$. The emitted intensity $I = I_1 + I_2$ can be found from Equation (10). The specific fluxes are strongly anisotropic at $\omega \ll \omega_B$. They have very sharp maxima along the local direction of the magnetic field, with a width $\Delta\vartheta \sim \sqrt{\omega/\omega_B}$, and, at some energies, broader maxima at intermediate angles. The beaming depends on the photon energy, just as the specific flux spectra depend on the direction of radiation (generally, on the angles ϑ, Θ and Θ_B). Some examples are provided by Shibanov *et al.* (1994) in this volume. The specific fluxes can be observed directly if the radiation is emitted from a small spot on the stellar surface. In particular, the properties of the specific fluxes should be used for light curve analysis and pulse-phase spectroscopy of the hard components of the ROSAT

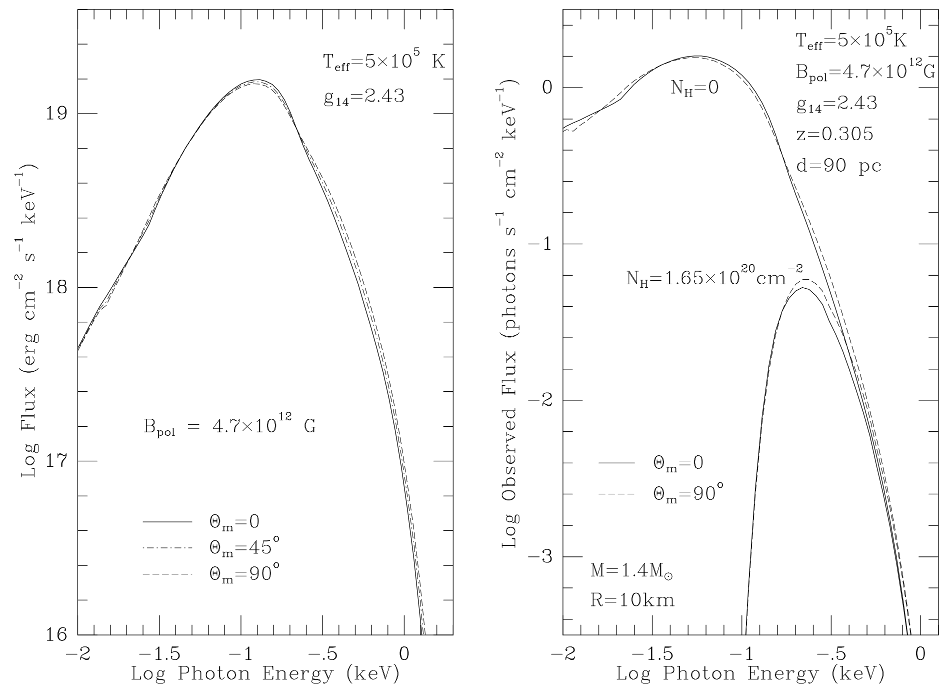

Fig. 6. **Left:** Energy flux spectra from the visible NS hemisphere of a NS with a dipole magnetic field. **Right:** Photon flux spectra as seen by an observer at the distance $d = 90$ pc.

spectra of NSs (see Section 1) if these components originate from hot polar caps on the NS surface. To describe the radiation from the stellar hemisphere, one should integrate the specific fluxes over the visible stellar surface. The resulting flux would coincide with the local fluxes (see Section 3.1) if the atmosphere parameters were uniform along the NS surface. Since, at least, the magnetic field varies along the surface, the flux from the visible hemisphere is generally different from any local flux, being dependent on the orientation of the NS magnetic axis with respect to the line-of-sight. An example of the surface-integrated fluxes emitted by a NS with a dipole magnetic field and a uniform effective temperature is shown in Figure 6. We see that the flux does depend on the angle Θ_m between the magnetic moment and line-of-sight, which means that the radiation of the rotating NS is pulsed even if the effective temperature is uniform. The pulsed fraction depends on the photon energy; its typical value in the soft X-ray range is $\sim 10\%$. There exists a crossover energy, ~ 0.2 keV in this example, at which the radiation is not pulsed at all. The pulses above and below this energy are phase-shifted by 180°. This example demonstrates

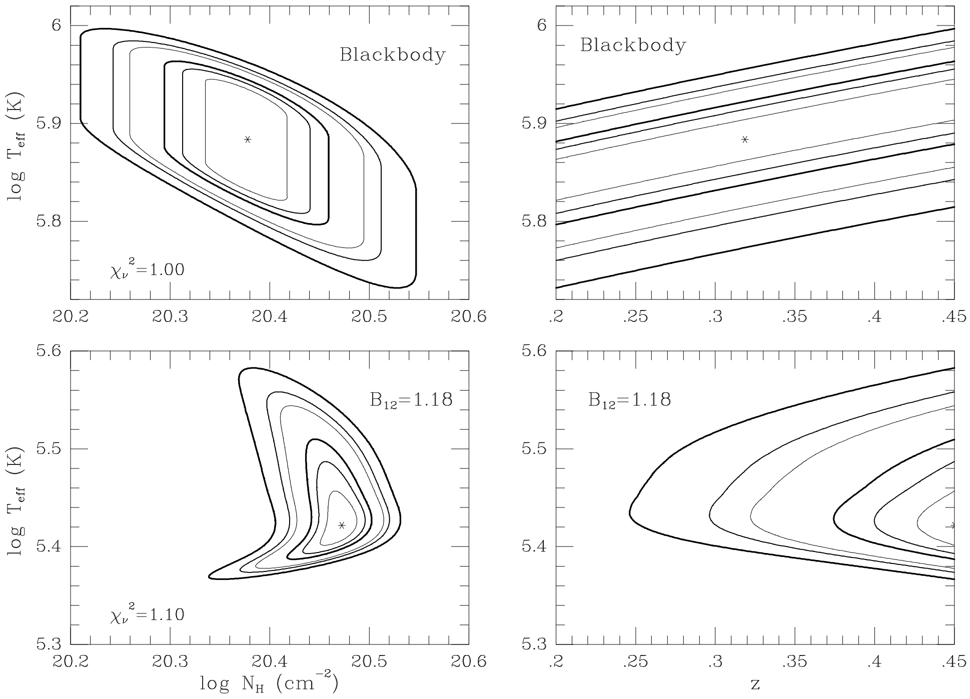

Fig. 7. Confidence contours for Geminga on the levels of 25%, 50%, 68.3%, 90%, 95% and 99%.

that the model NS surface radiation has all of the qualitative properties observed by ROSAT from several pulsars (Ögelman 1994). It should be noted that the value of the crossover energy and the pulsed fraction at different energies are both sensitive to polarizations of normal modes in the partially ionized atmosphere. (In this example, the polarizations were assumed to be exactly linear.) Moreover, even a very small nonuniformity of the effective temperature would shift the crossover energy and change the pulsed fraction. So, further investigations are necessary in order to apply the results to a detailed interpretation of the observational data.

4. DISCUSSION AND CONCLUSIONS

4.1. Observational implications

Since the model flux spectra differ substantially from the blackbody spectrum, fitting observed spectra to the atmosphere models will generally give results quite different from those of a blackbody fitting. To use the computed models for fitting, one should take into account the gravitational redshift $z = (1-2GM/Rc^2)^{-1/2}-1$ which depends on the NS mass and radius. One should also include the attenuation of the flux by interstellar absorption. The right panel of Figure 6 shows an example of the transformed photon number spectrum for $z = 0.305$ and for an effective hydrogen column density $N_H = 1.65 \times 10^{20}$ cm^{-2}. We see that for these typical parameters the photons near the maximum of the original spectrum are heavily absorbed, and the resulting spectrum has a maximum at $0.2 - 0.3$ keV.

The difference between the blackbody and atmosphere model fits is demonstrated in Figure 7 (see Meyer *et al.* 1994 for more details) which shows the confidence contours in the N_H-$T_{\rm eff}$ and z-$T_{\rm eff}$ planes obtained by fitting the soft spectral component of the radiation from Geminga observed by Halpern and Holt (1992) with the ROSAT PSPC. We fitted the time-integrated observed flux with a set of the model fluxes computed for $B = 1.18{\times}10^{12}$ G and $g = 2.43{\times}10^{14}$ cm s^{-2}. The fitting parameters in both the blackbody and the atmosphere fits are $T_{\rm eff}$, N_H and z. Fits to models with higher B give systematically larger χ^2. We see that, as expected, the atmosphere model fit results in an effective temperature which is a factor of $2-3$ lower than that obtained from the blackbody fit. The inferred temperatures lead to quite different conclusions about the cooling models. Generally, the atmosphere model fits are more compatible with fast cooling scenarios, and within these scenarios they imply much lower values of the critical temperature T_c of the superfluid transition for nucleons. For instance, if we adopt a model by Page and Applegate (1992), which allows cooling via the direct Urca processes for $M > 1.35M_\odot$, and assume $M = 1.4M_\odot$, then the blackbody fit would be consistent only with models for the neutron ${}^3P_2$ pairing which give the highest critical temperature, $T_c \sim 6 \times 10^9$ K. The model atmosphere fit yields much lower transition temperatures, $T_c \sim (0.8-0.9) \times 10^9$ K.

Applying the NS atmosphere models rather than a blackbody spectrum also allows one to possibly determine the gravitational redshift. We see from the z-$T_{\rm eff}$ contours that the atmosphere models give better fits for the highest z values ($z = 0.45$ in this example), whereas the blackbody fit can only give the ratio $T_{\rm eff}^\infty = T_{\rm eff}/(1+z)$, *i.e.*, the apparent "temperature at infinity". Measuring z gives additional information concerning the NS mass and radius. For instance, $z = 0.45$ would correspond to $M/M_\odot = 1.78(R/10\,{\rm km})$. In principle, one could additionally determine the best-fit gravitational acceleration g (if the data were of sufficiently high quality), which would allow one to find M and R separately.

4.2. Unsolved problems and further work

In this presentation we summed up the main results of the first generation of the cooling NS atmosphere models. However, many problems should still be solved to consider the subject fully investigated. Many of these problems deal with the properties of the compressed magnetized matter, in particular, with the opacity of the atomic fraction of the NS atmospheres. For instance, even in the simplest case of hydrogen atmospheres, we neglect the potentially important effect of the coupling of the center-of-mass motion of the atom to its internal structure (Vincke *et al.* 1992, Potekhin 1993). This coupling can significantly change the properties of the partially ionized gas (Pavlov and Mészáros 1993), including ionization equilibrium (Pavlov *et al.*, 1993) and the cross sections of bound-bound and bound-free transitions (Potekhin and Pavlov 1994, Bezchastnov and Potekhin 1993, Ventura *et al.* 1994). Incorporating this effect into the atmosphere models may lead to some distortion of the emitted spectra.

Another important problem concerns the contribution of the atomic fraction to polarizations of the normal modes (see Section 2.2). Although the polarizations should be almost linear, even a small admixture of the circular polarization can make a substantial effect on the opacity of the extraordinary mode, thus affecting the angular dependence of the outgoing radiation.

A number of problems are associated with high-density effects in the NS atmospheres. Although we included the most important nonideality effects into the ionization equilibrium and the bound-free opacities, some additional effects may still affect opacities in the most dense layers. For instance, we neglected Coulomb correlations of the charged particles, which may affect the distribution function of the electric microfields, the ionization equilibrium, and the equation of state. The high density also affects the propagation of photons when the frequency is lower than the electron plasma frequency; this may distort low-frequency regions of the spectra.

All of the results reported here were obtained for hydrogen atmospheres, which is probably justified by the gravitational stratification of the elements. It may happen, however, that hydrogen is virtually absent on certain NS surfaces. Obviously, other elements should be included in the models, and they may yield quite different spectra.

We have assumed radiative and hydrostatic equilibrium when computing the models. However, as one can see from Figure 4, the temperature gradients in some atmospheric layers gradually grow with decreasing effective temperature. In fact, our computations become unstable at $T_{\rm eff} \lesssim 2 \times 10^5$ K due to the steepness of the temperature profiles. This means that, perhaps, convective instability occurs at low $T_{\rm eff}$, and this should be incorporated into the modeling codes. Moreover, since the magnetic field is nonuniform along the NS surface and is not perpendicular to the surface, tangential components of the radiative flux (Kaminker *et al.* 1982b) may cause some flows (meridional circulation) in the atmosphere to maintain the heat balance. The meridional circulation can also be caused by an additional "magnetic force" exerted on the atoms in a nonuniform magnetic field (Pavlov and Mészáros 1993). These phenomena further complicate the investigation of NS atmospheres.

Acknowledgements

This research was partly supported through NASA grant NAGW-1522 and ESO C&EE grant No. A-01-068. We are indebted to the NATO ASI for support. We are grateful to J. Ventura, A. Potekhin and P. Mészáros for many useful dscussions.

References

Alcock, C., and Illarionov, A. F.: 1980, *Astrophys. J.*, **235**, 534.
Becker, W. and Trümper, J.: 1993, Nature, **365**, 528
Bezchastnov, V. G., and Potekhin, A. Yu.: 1993, *J. Phys. B*, submitted
Canuto, V., and Ventura, J.: 1977, *Fundam. Cosm. Phys.*, **2**, 203
Däppen, W., Anderson, L., and Mihalas, D.: 1987, *Astrophys. J.*, **319**, 195
Finley, J. P., Ögelman, H., and Kiziloğlu, Ü.: 1992, *Astrophys. J.*, **394**, L21

Forster, H., Strupat, W., Rösner, W., Wunner, G., Ruder, H., and Herold, H.: 1984, *J. Phys. B*, **17**, 1301
Gnedin, Yu. N., and Pavlov, G. G.: 1974, *Sov. Phys. JETP*, **38**, 903
Gnedin, O. Yu., and Yakovlev, D. G.: 1993, *Pis'ma Astron. Zh.*, **19**, 284
Gnedin, Yu. N., Pavlov, G. G., and Tsygan, A. I.: 1974, *Sov. Phys. JETP*, **39**, 301
Halpern, J. P., and Holt, S. S.: 1992, *Nature*, **357**, 222
Halpern, J. P., and Ruderman, M.: 1993, *Astrophys. J.*, **415**, 286
Herold, H., Ruder, H., and Wunner, G.: 1981, *J. Phys. B*, **14**, 751
Hummer D. G., and Mihalas, D.: 1988, *Astrophys. J.*, **331**, 794
Kaminker, A. D., Pavlov, G. G., Silant'ev, N. A. and Shibanov, Yu. A.: 1982a, *Astrofizika*, **18**, 283
Kaminker, A. D., Pavlov, G. G., and Shibanov, Yu. A.: 1982b, *Astrophys. Space Sci.* **86**, 249
Kaminker, A. D., Pavlov, G. G., and Shibanov, Yu. A.: 1983, *Astrophys. Space Sci.* **91**, 167
Khersonskii, V. K.: 1987, *Astron. Zh. (Sov. Astronomy)*, **64**, 433
Levenfish, K. P., and Yakovlev, D. G.: 1994, *Pis'ma Astron. Zh.*, **20**, 50
Lewin, W. H. G., Van Paradijs, J., and Taam, R. E.: 1992, *Space Sci. Rev.*, **62**, 223.
Mészáros, P.: 1992, *High-Energy Radiation from Magnetized Neutron Stars*, Univ. Chicago Press
Meyer, R.D., Pavlov, G.G., and Mészáros, P.: 1994, *Astrophys. J.*, in preparation
Mihalas, D.: 1978, *Stellar Atmospheres*, Freeman, San Francisco
Miller, M. C.: 1992, *Mon. Not. R. Astr. Soc.*, **255**, 109
Miller, M.C., and Neuhauser, D.: 1991, *Mon. Not. R. Astr. Soc.*, **253**, 107
Nomoto, N., and Tsuruta, S.: 1987, *Astrophys. J.*, **312**, 711
Ögelman, H. 1991, in *Neutron Stars: Theory and Observations*, p. 87, eds. J. Ventura and D. Pines, Kluwer (Dordrecht)
Ögelman, H.: 1994, this volume
Ögelman, H., and Finley, J. P.: 1993 *Astrophys. J.*, **413**, L31
Page, D.: 1993, *Astrophys. J.* (submitted)
Page, D., and Applegate, J. H.: 1992 *Astrophys. J.*, **394**, L17
Pavlov, G. G., and Mészáros, P.: 1993, *Astrophys. J.*, **416**, 752
Pavlov, G. G., and Panov, A. N.,: 1976, *Sov. Phys. JETP*, **44**, 300
Pavlov, G. G. and Shibanov, Yu. A. 1978, *Astron. Zh. (Sov. Astronomy)* **49**, 741
Pavlov, G. G., Shibanov, Yu. A., and Yakovlev, D. G.: 1980, *Astrophys. Space Sci.*, **73**, 33
Pavlov, G. G., Potekhin, A. Yu., Shibanov, Yu. A., and Zavlin, V. E.: 1993, presented at the NATO ASI *Lives of Neutron Stars* (Kemer, Turkey, Aug. 29 - Sep. 11, 1993)
Pethick, C. J.: 1992, *Rev. Mod. Phys.*, **64**, 1133
Potekhin, A. Yu.: 1993, *J. Phys. B*, submitted
Potekhin, A. Yu., and Pavlov, G. G.: 1993, *Astrophys. J.*, **407**, 330
Potekhin, A. Yu., and Pavlov, G. G.: 1994, in preparation
Shibanov, Yu. A., Zavlin, V. E., Pavlov, G. G., and Ventura, J. 1992 *Astron. Astrophys.*, **266**, 313
Shibanov, Yu. A., Zavlin, V. E., Pavlov, G. G., Ventura, J., and Potekhin, A. Yu.: 1993a, in *Isolated Pulsars*, p. 174, eds. K.A. Van Riper, R.I. Epstein, and C. Ho, Cambridge Univ. Press (Cambridge, UK)
Shibanov, Yu. A., Zavlin, V. E., Ventura, J., and Pavlov, G. G.: 1993b, in preparation
Shibanov, Yu. A., Zavlin, V. E., Pavlov, G. G., and Ventura, J.: 1994, this volume
Shibazaki, N. and Lamb, F. K.: 1989, *Astrophys. J.*, **346**, 808
Umeda, H., Shibazaki, N., Nomoto, K., and Tsuruta, S.: 1992, *Astrophys. J.*, **410**, 186
Van Riper, K. A., and Lattimer, J. M.: 1993, in *Isolated Pulsars*, eds. K. A. Van Riper, R. I. Epstein, and C. Ho, Cambridge Univ. Press (Cambridge, UK)
Ventura, J., Shibanov, Yu. A., Zavlin, V. E., and Pavlov, G. G.: 1993, in *Isolated Pulsars*, p. 168, eds. K. A. Van Riper, R. I. Epstein, and C. Ho, Cambridge Univ. Press (Cambridge, UK)
Ventura, J., Herold, H., and Kopidakis, N.: 1994, this volume
Vincke, M., Le Dourneuf, M., and Baye, D.: 1992, *J.Phys.B*, **25**, 2787
Yancopoulos, S., Hamilton, T. T., and Helfand, D.: 1993, *Astrophys. J.*, submitted
Zavlin, V. E., and Shibanov, Yu. A.: 1991, *Astron. Zh. (Sov. Astronomy)* , **68**, 999
Zavlin, V. E., Pavlov, G. G., and Shibanov, Yu. A.: 1993, in *Strongly Coupled Plasma Physics*, eds. H. M. Van Horn and S. Ichimaru, Univ. Rochester Press (Rochester)